# Sensitivity Assessment of a Microwave Apparatus for Breast Cancer Detection

| | |
|---|---|
| **Poster No.:** | C-1390 |
| **Congress:** | ECR 2018 |
| **Type:** | Scientific Exhibit |
| | |
|---|---|
| **Authors:** | G. Tiberi[1], L. Sani[1], N. Ghavami[2], M. Paoli[1], A. Vispa[1], G. Raspa[1], E. Vannini[1], A. Saracini[1], M. Duranti[1]; [1]Perugia/IT, [2]London/UK |
| | |
|---|---|
| **Keywords:** | Cancer, Instrumentation, Computer Applications-Detection, diagnosis, Experimental, Breast |
| **DOI:** | 10.1594/ecr2018/C-1390 |

# Aims and objectives

Microwave imaging has received increasing attention in the last decades, in particular for its breast cancer detection applications, encouraged by considerable difference between dielectric properties of malignant and normal tissues at microwave frequencies. Speci#cally, as shown in [1, 2], a signi#cant contrast between healthy breast tissue and malignant breast tissue is present; this contrast is shown to be up to a factor of 5 in conductivity and permittivity. Meanwhile, newer studies suggest the existence of this contrast only between fatty and malignant breast tissues, and a lower contrast (as low as 10% in dielectric properties) between healthy #bro glandular and malignant tissues [3-5].

Recently, a novel microwave apparatus (X-rays free mammogram, UBT Srl, Perugia, IT) has been constructed, tested and validated [6]. The apparatus, shown in Fig 1, operates in air, with 2 antennas, and uses a Huygens Principle based algorithm [7, 8] to generate images, which are homogeneity maps of tissues' dielectric properties. Huygens Principle based algorithm is able to capture the differences in dielectric properties (dielectric constant and/or conductivity) and discriminate between varying tissues, or various conditions of tissues, and depict this contrast through the resulting #nal image. For clarity, it is vital to emphasize that this apparatus is completely safe for both patients and operators, as it does not emit any ionizing radiation. In addition, the apparatus does not require any breast smashing.

Sensitivity of the apparatus is quantified here, after performing microwave imaging on 8 healthy and 12 non-healthy breasts (healthy and non-healthy breasts have been classified through a radiologist study).

**Images for this section:**

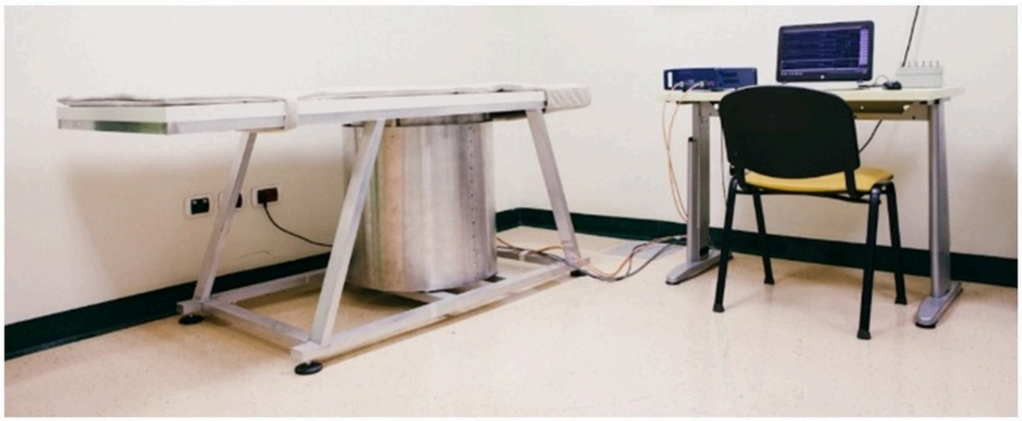

The microwave apparatus and the Vector Network Analyzer (VNA)

**Fig. 1:** The microwave apparatus (appropriately integrated in a bed) and the Vector Network Analyzer (driven by a processing unit). The microwave apparatus uses the Vector Network Analyzer as described in the next section.

# Methods and materials

***Clinical.***

We present the results of the first 16 volunteers who have been recruited and imaged under a protocol approved by the Ethical Committee of Regione Umbria, Italy (N. 6845/15/AV/DM of 14/10/2015, N. 10352/17/NCAV of 16/03/2017). The protocol concerns a feasibility study for detection of breast cancers using the proposed microwave mammogram apparatus, with the aim of quantifying the potential of the proposed microwave mammogram apparatus to be used for screening. The informed consent was obtained from all volunteers; moreover, 4 volunteers underwent the microwave imaging for the two breasts, and 12 volunteers underwent the microwave imaging for just one breast. All procedures performed in this study were in accordance with the ethical standards of the institutional and/or national research committee and with the 1964 Helsinki declaration and its later amendments or comparable ethical standards.

The radiologist study reviewed the conventional exam for each volunteer; conventional exam was constituted by echography and/or mammography or (limited to one case) magnetic resonance imaging. Echography was performed using the MyLab 70 xvg Ultrasound Scanner (Esaote, Genova, Italy); mammography was performed using Selenia LORAD Mammography System (Hologic, Marlborough, MA); magnetic resonance imaging was performed through a 3T scanner (Siemens Healthcare, Erlangen, Germany). The output of the radiologist study review is listed in Table 1, together with subjects' details. Specifically, where possible, the breast type has been classified according to its density, following the scale defined by the American College of Radiology (ACR) which goes from ACR1 (extremely fatty breast) to ACR4 (extremely heterogeneous fibroglandular breast) [9]. The inclusion type, if present, has been classified according to [10-12].

Once a subject agrees to participate in the protocol, the clinical study coordinator assists the subject with the positioning of her breast in the microwave apparatus. The exam data acquisition is completely computer controlled under the observation of a microwave system operator present in the room. Once the exam is completed, the data is transferred to a secure server for imaging.

***Microwave Apparatus.***

All microwave in-vivo images and results shown in this paper were reconstructed from data gathered using the apparatus installed at the Department of Diagnostic Imaging, Perugia Hospital, Perugia, Italy. The apparatus is constituted by one transmitting antenna (denoted here as TX) and by one receiving antenna (here denoted as RX). Both antennas operate in air, in the frequency band of 1 to 9 GHz. The apparatus is additionally constituted by: a hub with a cup that are placed to contain the breast of the patient (prone positioned) and two arms to rotatably associate TX and RX to the hub. The TX antenna is placed more radially external compared to the RX antenna. The RX antenna is placed more radially external with respect to the cup containing the breast. Both TX and RX antenna are con#gured to be rotated around the azimuth, such that they can pick up the re#ected electromagnetic #eld in all the different directions. Both antennas are connected to a Vector Network Analyzer VNA (Copper Mountain Technologies, IN, USA), which uses an output power of 1mW. Some details of the apparatus (appropriately integrated in a bed) are shown in Fig 2. For each TX and RX position, S21 was acquired at 1601 frequencies from 1 to 9 GHz in 5 MHz increments. TX and RX were positioned at the same height on the azimuth plane which crosses the centre of the breast of the prone subject (after checking that the half power beam angle of the antennas include the breast). On such azimuth plane, we used 15 transmitting positions, divided in 5 groups centred at 0°, 72°, 144°, 216°, 288°; each group contains 3 transmitting positions displaced 4.5° from each other. Moreover, we used 80 receiving positions displaced 4.5° from each other.

***<u>Microwave images.</u>***

To generate the image, the signals measured by the receiving antenna, i.e. the S21 output from the VNA, are processed by a processing unit through an imaging algorithm based on HP. We reconstructed the two-dimensional images in the azimuthal plane, i.e. coronal plane. In more details, we reconstructed images in a cylindrical grid with radius of 7 cm (equal to the receiving antenna radius). All images were acquired by employing (off-line) the imaging algorithm.

To be able to perform intra-breasts comparison, all intensity images have been normalized to unitary average. For each microwave image, we calculated the parameter Max/Avg (maximum of intensity divided by the average of intensity). Based on the classification performed by the radiologist, we calculated: the mean and standard deviation of Max/Avg for the healthy breasts; the mean and standard deviation of Max/Avg for the non-healthy breasts. We denoted with T the sum of mean and standard deviation of Max/Avg for the healthy breasts. Next, T has been used to classify the microwave images of non-healthy breasts. Specifically: if Max/Avg # T the image was classified as altered, while if Max/Avg < T the image was classified as non-altered.

## Images for this section:

| Subject index and breast (left/ right) | Year of birth | Breast Type | Diagnostic Test | Output of the radiologist study |
|---|---|---|---|---|
| 01R | 1983 | ACR4 | ecography | Healty |
| 01L | 1983 | ACR4 | ecography | Healty |
| 02R | 1936 | ACR2 | mammography | carcinoma papillary |
| 03R | 1960 | Not available | magnetic resonance | carcinoma infiltrating grade 2 |
| 04R | 1987 | ACR4 | ecography | Healty |
| 04L | 1987 | ACR4 | ecography | Healty |
| 05L | 1987 | Not available | ecography | benign fibroadenoma |
| 06L | 1975 | ACR2 | ecography + mammography | benign fibroadenoma |
| 07R | 1980 | ACR3 | ecography + mammography | benign microcalcifications |
| 08R | 1929 | ACR4 | ecography + mammography | carcinoma |
| 09R | 1963 | ACR3 | mammography | Healthy |
| 09L | 1963 | ACR3 | mammography | benign fibroadenoma |
| 10L | 1964 | ACR4 | mammography | Healthy |
| 10R | 1964 | ACR4 | mammography | Healthy |
| 11R | 1946 | ACR2 | mammography | Healthy |
| 12R | 1966 | ACR3 | mammography | carcinoma (4 cm), b5 |
| 13L | 1971 | ACR3 | mammography | carcinoma |
| 14L | 1996 | ACR3 | ecography | benign fibroadenoma |
| 15R | 1934 | ACR4 | Mammography | post surgical sieroma |
| 16R | 1969 | ACR4 | mammography | microcalcifications |

List of the subjects used for this study, each one with some details and the correspondent output of the radiologist study review. In summary, we have 8 healthy breasts and 12 non-healthy breasts; among the non-healthy breasts we also have a post-surgical breast with seroma.

**Table 1:** List of the subjects used for this study, each one with some details and the correspondent output of the radiologist study review.



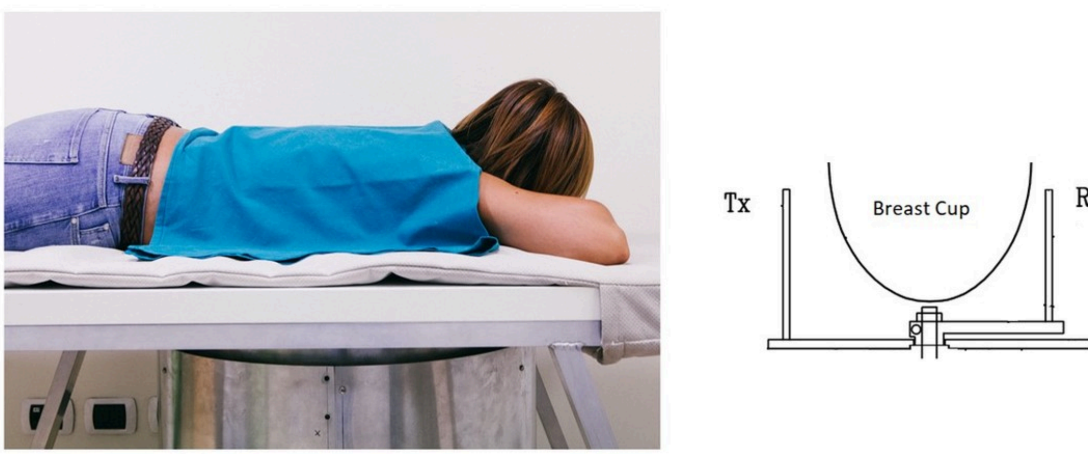


The microwave apparatus consists of a cup that holds the breast when the patient lies prone on the examination table. The transmitting (TX) and receiving (RX) antennas are located inside the hub and can be moved around the azimuth, to irradiate the breast (through TX) and capture the microwaves scattered by the breast itself (through RX). Both TX and RX are connected to a Vector Network Analyzer (VNA). No matching liquid is required

**Fig. 2:** The microwave apparatus consists of a cup that holds the breast when the patient lies prone on the examination table. The transmitting (TX) and receiving (RX) antennas are located inside the hub and can be moved around the azimuth, to irradiate the breast (through TX) and capture the microwaves scattered by the breast itself (through RX). Both TX and RX are connected to a Vector Network Analyzer (VNA). No matching liquid is required.

## Results

Fig 3 shows the microwave images obtained for subject 11R (a) and subject 08R (b); as pointed out before, to allow intra-subject comparison, the two images have been normalized to unitary average of the intensity. Axes are given in meter. Intensity is given in arbitrary unit, with a scale from 0 to 2. Microwave images are homogeneity maps of tissues' dielectric properties (both dielectric constant and conductivity), and are given here as 2D images in the azimuthal plane i.e. coronal plane. A certain level of in-homogeneity can be seen in both (a) and (b); however, in (b), in-homogeneity is more pronounced.

Figs 3c and 3d show the mammography images for subject 11R and 08R, mediolateral oblique views. Even if a co-registration between Fig 3b and Fig 3d is not possible, both figures detect an inclusion near the surface of the breast.

According to the radiologist study review, 8 healthy breasts and 12 non-healthy breasts underwent microwave imaging. For each microwave imaging exam, the parameter Max/Avg is given in Table 2; specifically, the left part of Table 2 refers to healthy breasts, while the right part of Table 2 refers to non-healthy breasts. For the healthy breasts, mean and standard deviation of Max/Avg are 1.64 and 0.04; for the non-healthy breasts, mean and standard deviation of Max/Avg are 1.77 and 0.09. The threshold T is equal to 1.68; T is then used to classify the microwave images of the non-healthy breasts. By comparing the output of the radiologist study with the classification of microwaves images performed using the threshold T, it is possible to note that 11/12 of non-healthy breasts have an altered microwave image; this turns out into a sensitivity of 91%.

## Images for this section:

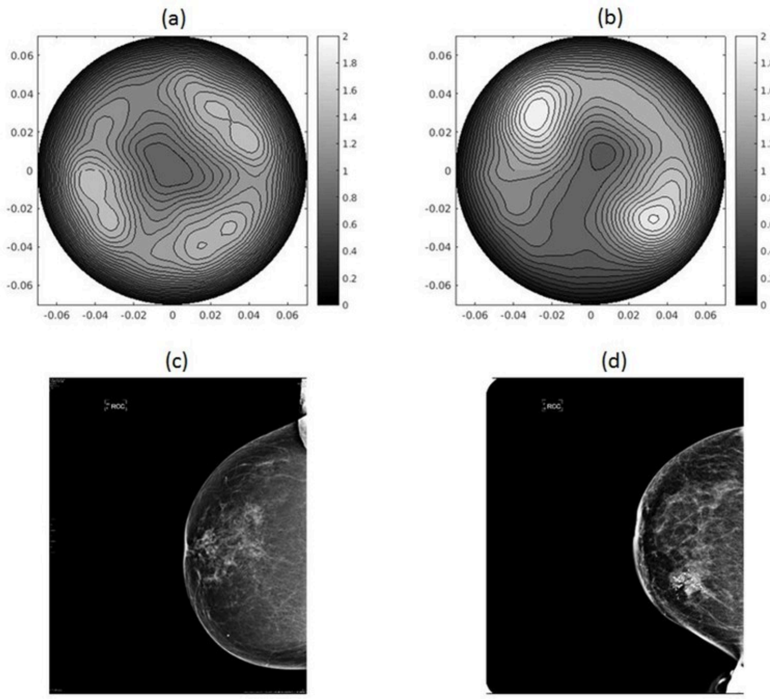


**Microwave images obtained for subject 11R (a) and subject 08R (b); to allow intra-subject comparison, the two images have been normalized to unitary average of the intensity. X and Y are given in meter. Intensity is given in arbitrary unit, with a scale from 0 to 2.**

**Mammography images for subject 11R (c) and 08R (d), mediolateral oblique views. Even if a co-registration between (b) and (d) is not possible, both figures detect an inclusion near the surface of the breast.**

**Fig. 3:** Microwave images obtained for subject 11R (a) and subject 08R (b). Mammography images for subject 11R (c) and 08R (d), mediolateral oblique views.



| Subject index and breast (left/ right) | Max/Avg of the microwave image |
|---|---|
| 01R | 1.66 |
| 01L | 1.67 |
| 04R | 1.68 |
| 04L | 1.68 |
| 09R | 1.64 |
| 10L | 1.66 |
| 10R | 1.63 |
| 11R | 1.54 |

*First column*: list of the healthy breasts according to the output of the radiologist study.
*Second column*: Max/Avg of the corresponding microwave images.

| Subject index and breast (left/ right) | Max/Avg of the microwave image | Microwave Images classification by using the threshold T |
|---|---|---|
| 02R | 1.74 | Altered |
| 03R | 1.78 | Altered |
| 05L | 1.72 | Altered |
| 06L | 1.71 | Altered |
| 07R | 1.69 | Altered |
| 08R | 1.98 | Altered |
| 09L | 1.72 | Altered |
| 12R | 1.65 | Not-Altered |
| 13L | 1.86 | Altered |
| 14L | 1.82 | Altered |
| 15R | 1.73 | Altered |
| 16R | 1.84 | Altered |

*First column*: list of the not-healthy breasts according to the output of the radiologist study.
*Second column*: Max/Avg of the corresponding microwave images.
*Third column*: classification of microwaves images performed using the threshold T.

**Table 2:** For each microwave imaging exam, the parameter Max/Avg (maximum of intensity divided by the average of intensity) is given.

# Conclusion

Images obtained using the proposed apparatus are intensity maps representing homogeneity of breast tissues' dielectric properties (dielectric constant and conductivity). Images obtained using the proposed apparatus can detect and locate mismatches in the region of transitions of the tissues. As the breast is constituted of non-homogeneous tissues, a certain level of mismatch can be also seen in the healthy breasts; such mismatch will be related to the subjects breast anatomy.

A classification of the mismatch in the microwave images can be performed through the parameter Max/Avg. Specifically, non-healthy breasts images have a mean Max/Avg approximately 10% greater than that of healthy breasts images. If we use T as threshold to classify microwave images, a sensitivity of 91% is achieved.

# Personal information

Dr. Gianluigi Tiberi, gianluigi@ubt-tech.com

UBT Srl

Spin Off of the University of Perugia

Via Santa Maria della Spina, 25

06081 Rivotorto di Assisi (PG)

ITALY

Dr. Michele Duranti, michele.duranti@ospedale.perugia.it

Department of Diagnostic Imaging, Perugia Hospital

Dipartimento di Diagnostica per Immagini e Laboratorio, Ospedale Santa Maria della Misericordia

06129 Perugia (PG)

ITALY

# References


[1] X. Li and S.C. Hagness, "A confocal microwave imaging algorithm for breast cancer detection", IEEE Microwave Wireless Comp. Lett., vol. 11, pp. 130132, Mar. 2001.

[2] E.J. Bond, X. Li, S.C. Hagness, B.D. Van Veen, "Microwave imaging via space-time beamforming for early detection of breast cancer", IEEE Transactions on Antennas and Propagation, Vol.: 51 , No. 8, Year: 2003, pp 1690 1705.

[3] N.K. Nikolova, "Microwave Imaging for Breast Cancer", IEEE Microwave Magazine, vol.12, no.7, pp.7894, Dec. 2011.

[4] M. Lazebnik, L. McCartney, D. Popovic, C.B. Watkins, M.J. Lindstrom, J. Harter, S. Sewall, A. Magliocco, J.H. Booske, M. Okoniewski , et al (2007a), "A large-scale study of the ultrawideband microwave dielectric properties of normal breast tissue obtained from reduction surgeries", Physics in medicine and biology 52(10):2637.

[5] M. Lazebnik, D. Popovic, L. McCartney, C.B. Watkins, M.J. Lindstrom, J. Harter, S. Sewall, T. Ogilvie, A. Magliocco, T.M. Breslin et al (2007b), "A large-scale study of the ultrawideband microwave dielectric properties of normal, benign and malignant breast tissues obtained from cancer surgeries", Physics in Medicine and Biology 52(20):6093

[6] G. Tiberi, R. Raspa, Apparatus for testing the integrity of mammary tissues, patent n. 0001413526.

[7] G. Tiberi, N. Ghavami, D.J. Edwards, A. Monorchio, "UWB Microwave Imaging of Cylindrical Objects with Inclusions", IET Microwaves, Antennas & Propagation, Volume: 5 , Issue: 12 Publication Year: 2011 , Page(s): 1440 1446.

[8] N. Ghavami, G. Tiberi, D.J. Edwards, A. Monorchio, "UWB Microwave Imaging of Objects With Canonical Shape", IEEE Transactions on Antennas and Propagation, Volume: 60 , Issue: 1, Publication Year: 2012 , Page(s): 231 239.

[9] American College of Radiology. Practice guidelines and technical standards. Reston, Va: American College of Radiology; 2008. ACR practice guideline for the performance of screening and diagnostic mammography.

[10] Tavassoli FA, Devilee P editors. World Health classification of Tumours. Pathology and genetics of tumours of the breast and female genital organs. IARC press, Lyon 2003.

[11] Lakhani S, Ellis IO, Schnitt SJ et al, editors. WHO classification of tumour of the breast, 4th edition. IARC: Lyon 2012.

[12] N. Perry, M. Broeders, C. de Wolf, S. Törnberg, R. Holland, L. von Karsa. European guidelines for quality assurance in breast cancer screening and diagnosis. Fourth Edition. European Commission 2006.